

Contents list available at **IJND**  
**International Journal of Nano Dimension**

Journal homepage: [www.IJND.ir](http://www.IJND.ir)

## Adsorption of Methyl orange dye from Water solutions by Carboxylate group functionalized multi-walled Carbon nanotubes

### ABSTRACT

**M. Rajabi<sup>1,\*</sup>**  
**O. Moradi<sup>2</sup>**  
**A. Mazlomifar<sup>1</sup>**

<sup>1</sup>Department of Chemistry,  
Shahre-Rey Branch, Islamic  
Azad University, Shahre-Rey,  
Tehran, Iran.

<sup>2</sup>Department of Chemistry,  
Shahre-Qods Branch, Islamic  
Azad University, Shahre- Qods,  
Tehran, Iran.

Received 19 April 2014  
Received in revised form  
24 June 2014  
Accepted 05 July 2014

The present study was carried out to investigate the potential of carboxylate group functionalized Multi-walled carbon nanotubes (MWCNT-COOH) adsorbent for the removal of Methyl orange (MO) textile dye from aqueous solutions. The effects of pH, shaking time and temperature on adsorption capacity were studied; the contact time to obtain equilibrium at 298 °K was fixed at 25 min. The effect of temperature on adsorption process was evaluated from 298 to 338 °K. Results showed that removal of Methyl orange increased with increasing contact time and decreased with increasing pH and temperature. For Methyl orange dye, the equilibrium data were best fitted to The Langmuir isotherm model. The adsorbent was characterized by infrared spectroscopy, and scanning electron microscopy. The pseudo-second-order kinetic model provided the best fit to the experimental data compared with The Elovich or pseudo-first-order or intra-particle diffusion kinetic adsorption models.

**Keywords:** Adsorption; Dye; MWCNT-COOH; Methyl orange; Aqueous solutions.

### INTRODUCTION

Dyeing operation in textile industries uses large amounts of water and generates high volumes of coloured wastewaters. A fair estimative of dye losses to the environment is about 1-2% during their production and 1-10% in their use [1]. Effluents from the textile industry contain various kinds of synthetic dyestuffs, and there has been increasing scientific interest in regard to decolorization of these effluents in the last few decades [2]. Dyes can cause allergy, dermatitis, skin irritation [3] and also provoke cancer [4] and mutation in humans [5].

Textile dyeing effluents are composed by complex mixtures of dyes, auxiliary chemicals, salts, acids, bases, organochlorinated compounds and occasionally heavy metals [6].

\* Corresponding author:  
Mostafa Rajabi  
Department of Chemistry, Shahre-Rey Branch, Islamic Azad University, Shahre-Rey, Tehran, Iran.  
Tel +982133583363  
Fax +9821 33586107  
Email  
[mostafa\\_moshavere@yahoo.com](mailto:mostafa_moshavere@yahoo.com)

Colour removal is, however, one of the main problems in the treatment of this kind of effluents, due to dye resistance to biodegradability, light, heat and oxidizing agents [7]. Traditional treatments involving biological and coagulation/flocculation methods are generally ineffective for total colour removal. A wide range of other methods has been developed, like adsorption on organic and inorganic matrices, photocatalysis, chemical oxidation, microbiological or enzymatic decomposition, etc. [8].

Bottom ash and deoiled soya were used as adsorbents for the removal of basic fuchsin and azo dye acid orange. Activated carbon and activated rice husks were used for the adsorption of safranin-T from wastewater. Carbon slurry developed from a waste material has been used for the removal of endosulfan and methoxychlor and vertigo blue 49 and orange DNA13 from water. An agricultural waste, wheat husk, was used for the removal of golden yellow 3 RFN from aqueous solution. However, the adsorption process has the major drawback of requiring disposal of the resulting sludge residue. Methods by which the adsorbed pollutants can be degraded are required [9].

Carbon nanotubes (CNTs) have attracted great attention in multidisciplinary areas due to their unique hollow tube structure and their many outstanding mechanical, electronic and optical properties [10]. In comparison with classical adsorbents such as activated carbon and clay, CNTs is more attractive because of its favorable physicochemical stability, high selectivity, and structural diversity. Extensive experiments have been conducted on the adsorption of inorganic or organic contaminants on CNTs such as  $\text{Zn}^{2+}$  [11],  $\text{Cd}^{2+}$  [12],  $\text{Pb}^{2+}$  [13],  $\text{Cu}^{2+}$  [14],  $\text{Cr}^{6+}$  [15], fluoride [16] and dioxin [17].

## EXPERIMENTAL

### Solutions

De-ionized water was used throughout the experiments for solution preparation. The textile dye, Methyl orange (MO;  $\text{C}_{14}\text{H}_{14}\text{N}_3\text{Na}_3\text{O}_5\text{S}$ ; 327.34 g/mol) was from the commercial manufacturing company DyStar Co. (Germany) at 90% purity. The dye was used without further purification. The MO dye has one sulphat group

(see Supplementary Figure 1). These groups present negative charges even in highly acidic solutions due to their  $\text{pK}_a$  values lower than zero [18]. The stock solution was prepared by dissolving the dye in distilled water to a concentration of  $50.00 \text{ g L}^{-1}$ . Working solutions were obtained by diluting the dye stock solutions to the required concentrations. To adjust the pH of the solutions,  $0.10 \text{ mol L}^{-1}$  sodium hydroxide or hydrochloric acid were used. The pH of the solutions was measured using a Schott Lab 850 set pH meter.

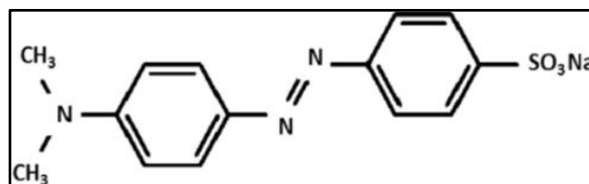


Fig. 1. Structure of methyl orange (MO).

### Adsorbent

MWCNT -COOH (content of COOH, 6 wt%; with purity > 95%; average diameter 1-2 nm; length 530 nm and SSA  $\sim 400 \text{ m}^2/\text{g}$ ) were prepared by catalytic chemical vapor deposition (CVD). The MWCNT-COOH adsorbent was characterized by vibrational spectroscopy in the infrared region with Fourier Transform (FTIR) using a Varian spectrometer, model 640-IR. The spectra were obtained with a resolution of  $500 \text{ cm}^{-1}$  with 4000 cumulative scans. For area the adsorbent samples were also analyzed by scanning electron microscopy (SEM) in a KYKY microscope, model EM 3200 [19].

### Adsorption studies

Adsorption studies for the evaluation of the MWCNT-COOH adsorbent for the removal of the MO dye from aqueous solutions were carried out in triplicate using the batch contact adsorption method. For these experiments, 20.0 mg of adsorbent placed in 100.0 mL flasks containing 20.0 mL of the dye solution ( $10.0\text{--}50.0 \text{ mg L}^{-1}$ ) [20], which were agitated for a suitable time (5 min to 45 min in the kinetic experiments; and 25 min in the equilibrium isotherms) at different temperatures ( $298\text{--}338 \text{ K}$ ). The pH of the dye solutions ranged from 2.0 to 10.0. Subsequently, in order to separate the adsorbent from the aqueous solutions, the flasks were centrifuged at 4,500 rpm for 5 min using a

centrifuge model; 5702R (Pendorf, Germany) in the equilibrium isotherm or filtered in a (0.2  $\mu\text{m}$ ) membrane in the kinetic experiments, and aliquots of 1-10 mL of the supernatant were properly diluted with an aqueous solution fixed at a suitable pH value.

The final concentrations of the dye which remained in the solution were determined by visible spectrophotometry using a UV-VIS spectrophotometer furnished by Varian (Cary 100 Bio) (London-England) provided with quartz optical cells. Absorbance measurements were made at the maximum wavelength of MO dye at 480 nm. The amount of dye taken up and the percentage of removal of the dye by the adsorbent were calculated by applying Eqs. (1) and (2), respectively:

$$q = \left( \frac{C_0 - C_e}{m} \right) \times V \quad (1)$$

$$\% \text{Removal} = 100 \times \frac{(C_0 - C_e)}{C_0} \quad (2)$$

Where  $q$  is the amount of dye taken up by the adsorbent ( $\text{mg g}^{-1}$ ),  $C_0$  is the initial dye concentration put in contact with the adsorbent ( $\text{mg L}^{-1}$ ),  $C_e$  is the dye concentration ( $\text{mg L}^{-1}$ ) after the batch adsorption procedure,  $m$  is adsorbent mass (g) and  $V$  is the volume of the dye solution (L). The experiments of desorption were carried out according to the procedure: A 30.0 ( $\text{mg L}^{-1}$ ) of MO dye was shaken with 20.0 mg of MWCNT-COOH for 25 min. Then, upon completion, the sample of the mixture was removed from the flask and separated by centrifuging at 4,500 rpm for 5 min. The obtained solution was later analyzed for residual MO. To evaluate the fitness of kinetic and

isotherm equations to the experimental data, the chi-square statistic ( $X^2$ ) was used to measure the kinetic and isotherm constants [10, 21-31].  $X^2$  can be defined as:

$$X^2 = \sum_i^N \frac{(q_{e,\text{exp}} - q_{e,\text{cal}})^2}{q_{e,\text{cal}}} \quad (3)$$

If data from the model are similar to the experimental data,  $X^2$  will be a small number; if they are different,  $X^2$  will be a large number. The subscripts "exp" and "calc" show the experimental and calculated values and  $N$  is the number of observations in the experimental data.

### Kinetic and equilibrium models and its statistical evaluation

The Elovich [10], pseudo-first-order [32], pseudo-second-order [33] and intra-particle diffusion [34]. The Langmuir [35], Freundlich [36] isotherm equations are given in Supplementary Table 1 and Table 2. The kinetic and equilibrium models were fitted by employing a linear method. The adsorption isotherm indicates how the adsorbate molecules are distributed between the liquid phase and the solid phase when the adsorption process reaches an equilibrium state. In other words, adsorption isotherm is basically important to describe how solutes interact with adsorbent, and it is also crucial in optimizing the usage of adsorbent [37-39]. Which measured the differences in the amount of dye taken up by the adsorbent predicted by the models and the actual  $q$  measured experimentally; the chi-square statistic ( $X^2$ ) was used to measure the kinetic and isotherm constants [10].

**Table 1.** Langmuir isotherm parameters and ARE parameter for adsorption of MO dye on MWCNT-COOH. Conditions:  $C_0$ : 10-50 mg/ L of dye solution; mass of adsorbent: 20 mg; the temperature: 298 K and time: 25min at pH 2.

Langmuir Type	Equation	K(L/mg)	Qm(mg/g)	R <sup>2</sup>	X <sup>2</sup>	R <sub>L</sub>
Type1	$\frac{C_e}{q_e} = \frac{1}{KQ_m} + \frac{C_e}{Q_m}$	0.495	5.580	0.987	3.40	0.06 – 0.67
Type2	$\frac{1}{q_e} = \frac{1}{Q_m} + \frac{1}{KQ_mC_e}$	0.424	5.050	0.996	2.98	
Type3	$q_e = Q_m \frac{q_e}{KC_e}$	0.016	5.695	0.998	2.21	
Type4	$\frac{q_e}{C_e} = KQ_m - Kq_e$	0.016	5.750	0.996	2.44	

**Table 2.** The pseudo second-order kinetic parameters for MO removal using MWCNT-COOH adsorbent and the calculation of activation energy ( $E_a$ ) for the adsorption process using the Arrhenius equation. Conditions:  $C_0$ :20mg/ L of dye solution; mass of adsorbent: 20 mg; the temperature: 298 K and time: 5-45 min at pH 2.

Kinetic model	T(K)	$K_2(\text{min}^{-1})$	$R^2$	$X^2$	A	$E_a(\text{kJ/mol})$
The pseudo second-order	298	$3.63 \times 10^{-2}$	0.999	0.8	0.555	0.029
	308	$3.61 \times 10^{-2}$	0.998	1.2		
	318	$3.58 \times 10^{-2}$	0.998	1.1		

## RESULTS AND DISCUSSION

### Characterization of the adsorbents

The FTIR technique was used to examine the surface groups of adsorbent (MWCNT-COOH) and to identify the groups responsible for dye adsorption. Infrared spectra of the adsorbent and dye-loaded adsorbent sample, before and after the adsorption process, were recorded in the range 4000-500  $\text{cm}^{-1}$  (Figure 2). After the adsorption procedure, the functional groups that interact with the dye suffered a shift to lower wavenumbers when the adsorbate withdrew electrons of the adsorbent group. On the other hand, when the adsorbate furnished electrons to the adsorbent, the FTIR vibration bands shifted to higher wavenumbers [21]. Figure 2 A and B shows the FTIR vibrational spectra of the MWCNT-COOH before the adsorption and loaded with the dye Methyl orange (MWCNT-COOH + MO) after the adsorption, respectively. The intense absorption bands at 3438 and 3433  $\text{cm}^{-1}$  were assigned to (O-H) bond stretching, before and after interaction, respectively [21,22] indicating that this group plays a role in the adsorption of the MO dye. The ( $\text{CH}_2$ ) stretching bands at 2924 and 2856  $\text{cm}^{-1}$  were assigned of ( $\text{CH}_2$ ) groups [21, 22], respectively, which presented the same wavenumbers before and after adsorption, indicating that these groups did not participate in the adsorption process [23]. Small bands at 1726 and 1731  $\text{cm}^{-1}$ , before and after absorption, respectively, were assigned to the carboxyl groups ( $\text{C}=\text{O}$ ) of carboxylic acid ( $\text{COOH}$ ) [21, 22]. Reaction of the MO dye with the MWCNT-COOH should also occur by the  $\pi$ - $\pi$  interaction of the dye with the aromatic rings of the carbon nanotube [21], in addition to interactions

with other functional groups (OH, COOH). In addition, strong bands at 1180 and 1097  $\text{cm}^{-1}$  before and after adsorption, respectively, confirmed the presence of a C-O bond (Figure 2B) [21,22], reinforcing the interaction of the dye with carboxylate groups. Based on the FTIR bands, it could be concluded that the adsorption of MO dye on MWCNT-COOH occurred mainly on the groups OH, COOH and at the aromatic rings.

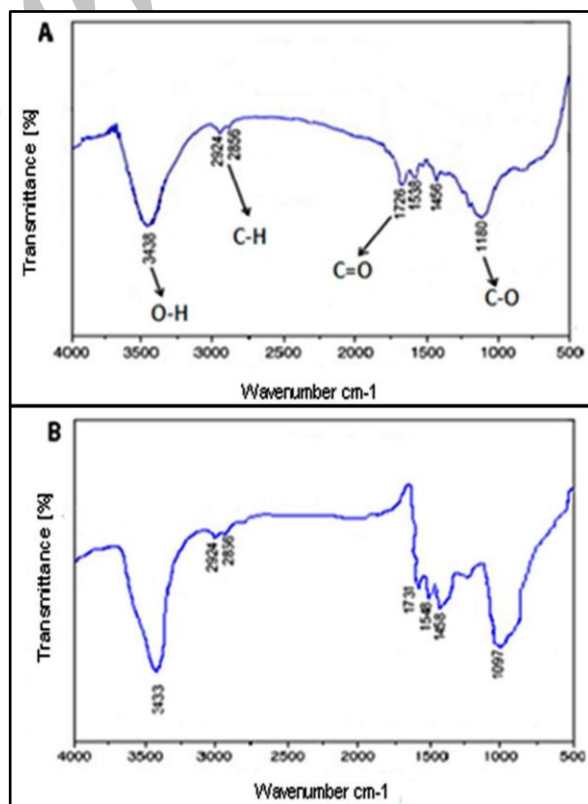


**Fig. 2.** Infrared spectra of adsorbent: (A) MWCNT-COOH, (B) MWCNT + MO.



Scanning electron microscopy of the adsorbent is presented on Figure 3. These micrographs suggest that MWCNT-COOH could be expanded when immersed in aqueous solution, because this adsorbent is an entanglement of carbon tubes [38]. Since it has been reported in the literature [23], the PAC material is a more compact material, which is composed of carbon fragments.

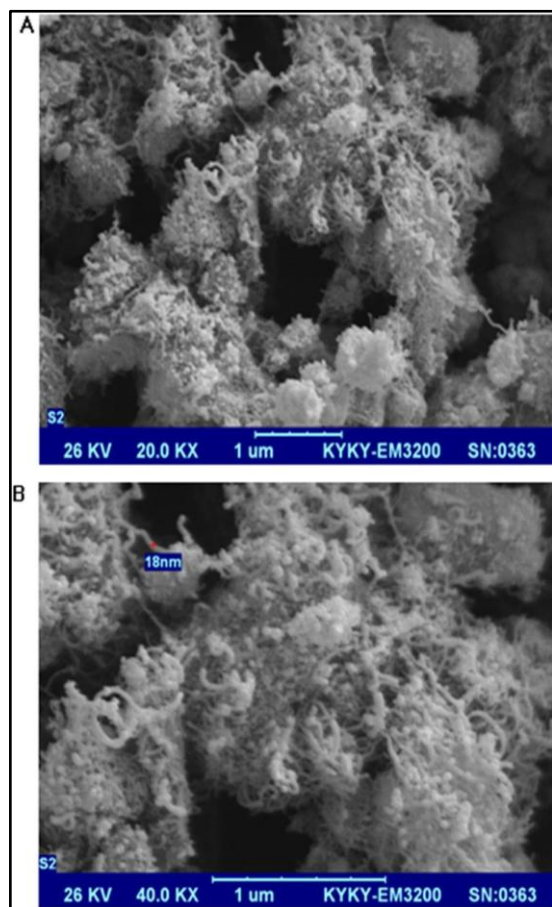


**Fig. 3.** SEM of adsorbent. (A) MWCNT-COOH + MO (magnification 20,000 $\times$ ), (B) MWCNT-COOH + MO (magnification 40,000 $\times$ ).

### Effects of pH on adsorption

One of the most important factors in adsorption studies is the effect of acidity on the medium [27]. Different species may present divergent ranges of suitable pH depending on which adsorbent is used. The effects of initial pH on the percentage of removal of the MO dye using MWCNT-COOH adsorbent were evaluated within the pH range between 2 and 10 (Figure 4). The percentage of dye removal decreased from pH 2.0 up to 10.0. For MWCNT-COOH adsorbent, the

decrease in the percentage of dye removal when the pH ranged from 2.0 to 10.0 was 90.71% and 32.43%, respectively.

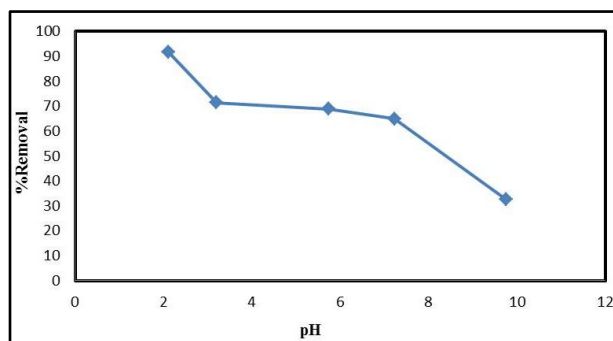


**Fig. 4.** Effect of pH on the adsorption of MO dye on MWCNT-COOH. Conditions:  $C_0$ : 20 mg/L of dye solution; mass of adsorbent: 20 mg; the temperature: 298 K and time: 25 min.

The  $pH_{pzc}$  values determined for MWCNT-COOH adsorbent was 5.85, respectively. For pH values lower than  $pH_{pzc}$ , the adsorbent presents a positive surface charge [10, 31]. The dissolved MO dye is negatively charged in water solution, because it possesses sulphat group [27]. The adsorption of this dye takes place when the adsorbent present a positive surface charge. For MWCNT-COOH, the electrostatic interaction occurs for  $pH < 6.85$ , respectively. However, the lower the pH values from the  $pH_{pzc}$ , the more positive the surface of the adsorbent [10, 32]. This behaviour explains the high adsorption capacity of adsorbent for the MO dye at pH 2. In order to continue the adsorption studies, the initial pH was fixed at 2.0. It should be stressed that the final pH of the adsorbate solution after the adsorption procedure did not changed remarkably. The final pH values of the adsorbate solutions were measured and its values attained up to 2.2.

### Effect of contact time

In order to determine the contact time is required for the adsorption of Mo on MWCNT-COOH, 20 ml, 30 mg/L solution was shaken with 20 mg MWCNT-COOH. The equilibrium studies were performed at the selected intervals of time ranging from 5 to 45 min. As shown in Figure 5A; after 25 min stirring of the solution, the removal efficiency did not increase. Therefore, the optimum value of stirring time was found to be 25 min. The change in the rate of MO dye removal might be due

to the fact that initially all adsorbent sites were vacant and the solute concentration is high. Afterward the MO dye uptake rate by the MWCNT-COOH decreased significantly due to the decrease in vacant adsorption sites. On the basis of these results, a 25 min shaking period was selected for all further studies.

#### Effect of temperature on adsorption

The effect of temperature was studied at 298-338 °K with 20 ml, 30 mg/L MO dye solution and 20mg g MWCNT-COOH. As shown in Figure 5B. Results showed that removal of Methyl orange decreased with temperature increasing.

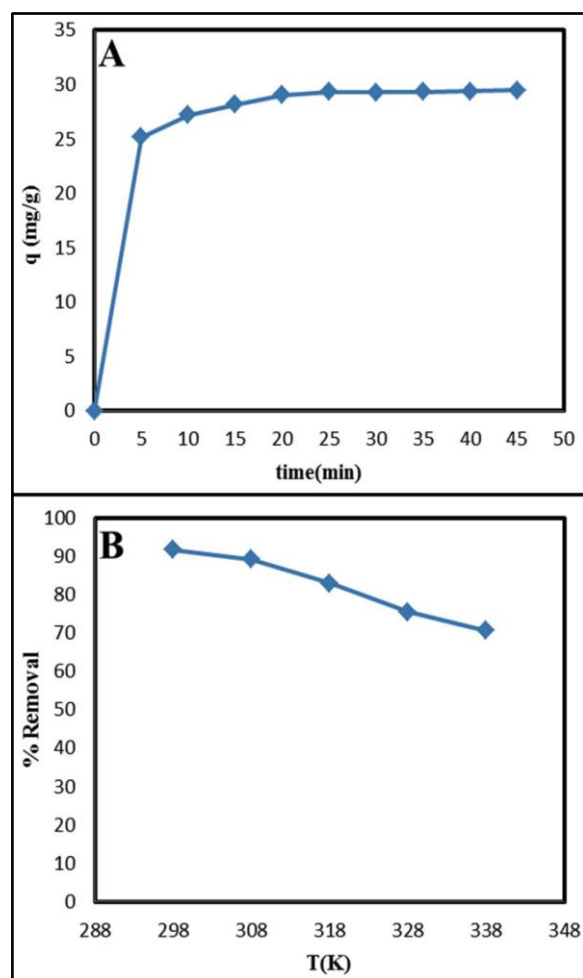


**Fig. 5.** (A) Effect of contact time on the percentage of removal of the MO dye using MWCNT-COOH adsorbent. Conditions:  $C_0$ :20mg/ L of dye solution; mass of adsorbent: 20 mg; the temperature: 298 K at pH 2.(B) Effect of temperature on the percentage of removal of the MO dye using MWCNT-COOH adsorbent. Conditions:  $C_0$ :20mg/ L of dye solution; mass of adsorbent: 20 mg and time: 25min at pH 2.

#### Effect of initial methyl orange concentration

The effect of initial Methyl orange dye concentration was studied at different initial MO dye concentrations in the range of 10-50 mg/L at 298 K with 0.02 g MWCNT-COOH at 25 min. MO dye adsorption capacity increased with increasing initial MO dye concentration in solution. This can be attributed to the fact that Electrostatic repulsion between the negatively charged methyl orange (Figure 1) and negative Surface charge of MWCNT-COOH [23] to create conditions unfavorable for sorption and reduce adsorption MO dye on MWCNT-COOH.

#### Equilibrium studies

The isotherms of adsorption were carried out with MO dye on the MWCNT-COOH adsorbent (see Figure 6). Based on the  $X^2$ , the Langmuir model was the best isotherm model for adsorbent at all the initial Methyl orange dye concentrations studied. The Langmuir model showed (Table 1) the lowest  $X^2$  values, which means that the  $q$  fit by the isotherm model was close to the  $q$  measured experimentally. The Freundlich, Temkin, Dubinin-Radushkevich and Halsey isotherm models were not suitably fitted, presenting  $X^2$  values ranging from 3.77 to 51.4-fold and from 2.31 to 56.1-fold higher than the  $X^2$  values obtained by the Langmuir isotherm model, using MWCNT-COOH as adsorbent, respectively. By this reason, the isotherm parameters of the Freundlich, Temkin, Dubinin-Radushkevich and Halsey were not presented on Table 1 because these values have no physical meaning.

- **Langmuir isotherm**

One of the most common isotherm models which are widely used is the Langmuir model. It is observed that the Langmuir isotherms can be linearized to at least four different types. The Langmuir isotherm model can be expressed as:

$$q_e = \frac{Q_m K C_e}{(1 + K C_e)} \quad (4)$$

Where  $Q_m$  (mg/g) and  $K$  (L/mg) are Langmuir constants related to adsorption capacity and energy of adsorption, respectively [35]. The essential characteristics of a Langmuir isotherm can be expressed in terms of a dimensionless separation

factor;  $R_L$  which describes the type of isotherm and is defined by [40-43]:

$$R_L = \frac{1}{(1+KC_0)} \quad (5)$$

If  $R_L > 1$ , unfavorable;  $R_L = 1$ , linear;  $0 < R_L < 1$ , favorable;  $R_L = 0$ , irreversible.

The  $R_L$  parameter lies between 0.06 and 0.67 which proves that the adsorption process is favorable MWCNT-COOH is a potential adsorbent for the removal of MO dye from aqueous solution. The Langmuir plots for MO dye adsorption on MWCNT-COOH were obtained and shown in Figure 6. Table 1 summarizes the correlation coefficients of Langmuir isotherm.

- **Freundlich isotherm**

Freundlich isotherm usually gives good curve fitting over a wider adsorbate concentration range, but its constants provide little physical

insights into the adsorption mechanism. The values of these constants vary markedly with adsorbate concentration. It can be expressed as:

$$q_e = K_F C_e^{1/n} \quad (6)$$

Where,  $K_F$  and  $1/n$  are the Freundlich constants [36]. Similarly the Freundlich isotherm constants  $K_F$  and  $1/n$  which are indicators of adsorption capacity and adsorption intensity, respectively, could be calculated from the plot of  $\ln q_e$  versus  $\ln C_e$ . The results are provided in Figure 7. The magnitude of  $1/n$  quantifies the favorability of adsorption and the degree of heterogeneity on the surface of MWCNT-COOHs. If  $1/n$  has a value less than unity suggesting favorable adsorption, adsorption capacity increases and new adsorption sites form [44].

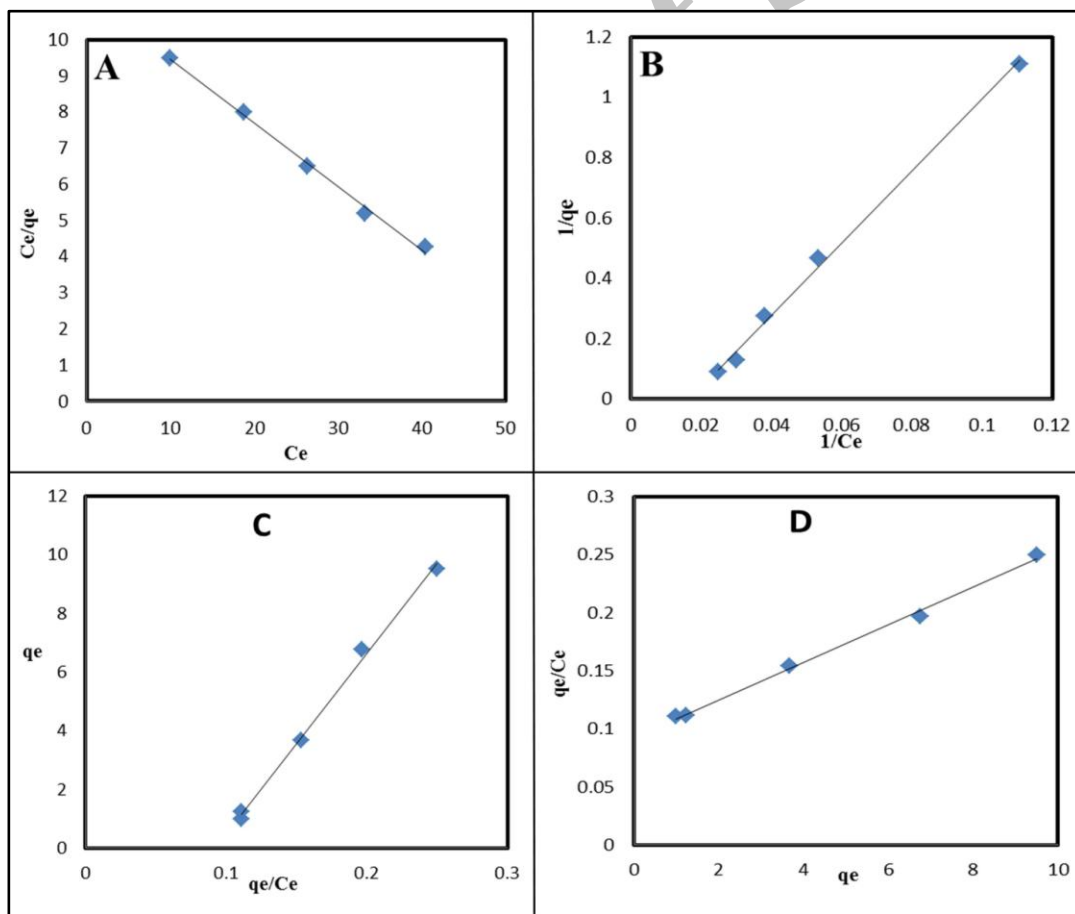


**Fig.6.** Langmuir isotherm model of MO dye on MWCNT-COOH surface (A) Type (I) of Langmuir; (B) Type (II) of Langmuir; (C) Type (III) of Langmuir and (D) Type (IV) of Langmuir. Conditions:  $C_0$ :10-50 mg/ L of dye solution; mass of adsorbent: 20 mg; the temperature: 298 K and time: 25min at pH 2.

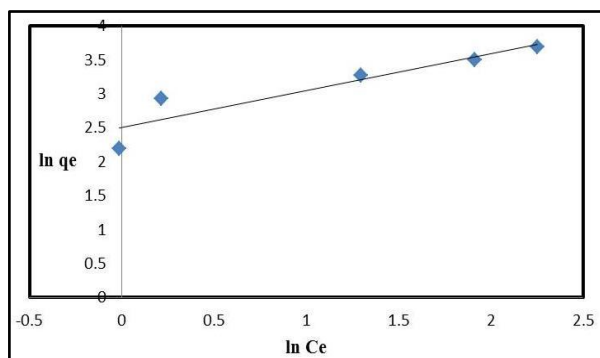


**Fig. 7.** Freundlich adsorption isotherms of MO dye on MWCNT-COOH. Conditions:  $C_0$ : 10-50 mg/L of dye solution; mass of adsorbent: 20 mg; the temperature: 298 K and time: 25 min at pH 2.

- **Temkin isotherm**

Temkin isotherm model describes the behavior of adsorption systems on a heterogeneous surface, and can be expressed as:

$$q_e = B \ln (A C_e) \quad (7)$$

where  $B$  is a constant related to adsorption heat and is equal  $RT/b$ ,  $A$  is the equilibrium binding constant corresponding to maximum to binding energy [45]. As shown in Figure 8B the plot of  $q_e$  versus  $\ln C_e$  was used to determine isotherm constants.

- **Dubinin-Radushkevich isotherm**

The Dubinin-Radushkevich (D-R) equation is given as

$$q_e = X'_m \exp (-K' \varepsilon^2) \quad (8)$$

Where  $q_e$  is the amount of MO dye adsorbed per unit mass of MWCNT-COOH adsorbent,  $X'_m$  is adsorption capacity,  $K'$  is a constant related to adsorption energy [39],  $\varepsilon$  is Polanyi potential and can be correlated as:

$$\varepsilon = RT \ln(1 + \frac{1}{C_e}) \quad (9)$$

$R$  is the gas constant and  $T$  is adsorption temperature.  $K'$  gives the mean free energy  $E$  of sorption per molecule of adsorbate when it is transferred to the surface of the solid from infinity in the solution and can be calculated using the following equation [39]:

$$E = \frac{1}{\sqrt{-2K'}} \quad (10)$$

The values of  $X'_m$  and  $K'$  were calculated from the intercept and slope of the  $\ln q_e$  versus  $\varepsilon^2$  plots as shown in Figure 8C.

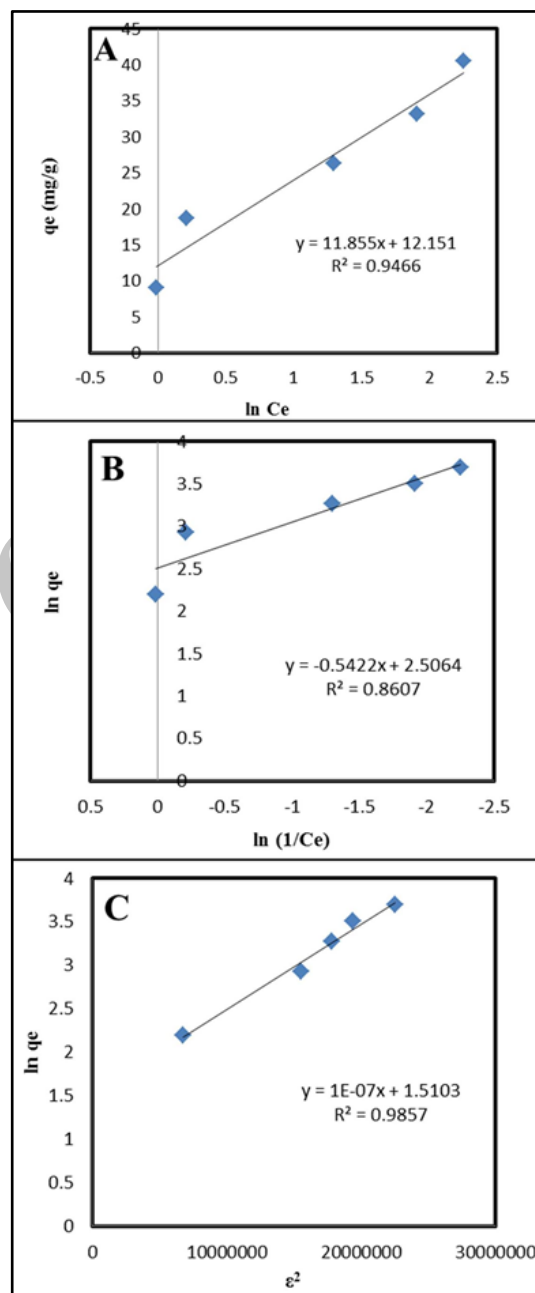


**Fig.8.** (A) Temkin adsorption isotherm of MO dye on MWCNT-COOH (B) Halsey adsorption isotherm of MO dye on MWCNT-COOH (C) Dubinin-Radushkevich (D-R) adsorption isotherm of MO dye on MWCNT-COOH. Conditions:  $C_0$ : 10-50 mg/L of dye solution; mass of adsorbent: 20 mg; the temperature: 298 K and time: 25 min at pH 2.



- **The Halsey isotherm**

The Halsey [39] adsorption isotherm can be given as:

$$\ln q_e = \left[\left(\frac{1}{n}\right) \ln K\right] - \left(\frac{1}{n}\right) \ln C_e \quad (11)$$

This equation is suitable for multilayer adsorption. Especially, the fitting of this equation can be best used for heterotopous solids. Curve of  $\ln q_e$  versus  $\ln C_e$  Halsey adsorption isotherm are given in Figure 8B.

### Kinetic studies

Adsorption kinetic studies are important in the treatment of aqueous effluents because they provide valuable information on the mechanism of the adsorption process [27]. It is important to point out that the initial MO concentration employed during the kinetic studies was (30.0 mg L<sup>-1</sup>) when compared with other studies reported in the literature [10,23,24]. MWCNT adsorbent has very high adsorption capacity and adsorb practically all the MO dye when the initial adsorbate concentrations are lower than 150 mg L<sup>-1</sup>. In attempting to describe the adsorption kinetics of MO dye using the MWCNT-COOH adsorbent, four kinetic models were tested, as shown in Figure 9. Pseudo Second-order Model, kinetic parameters are listed in Table 2 for MWCNT-COOH. The Elovich, and pseudo-first order, and Intra-particle Diffusion kinetic models were not suitably fitted (see Figure 9) and by this reason these values were not reported on Table 2, because these parameters have no physical meaning. Therefore, the kinetic data were only suitably fitted by the Pseudo Second-order kinetic model that presented low X<sup>2</sup> values and also high R<sup>2</sup> values.

- **Elovich Model**

The Elovich model equation is generally expressed as [40]:

$$\frac{dq_t}{dt} = \alpha \exp(-\beta q^2) \quad (12)$$

To simplify the Elovich equation, Chien and Clayton assumed  $\alpha, \beta \gg t$  and by applying the boundary conditions at  $t = 0$  and at equation (12) become  $q_t = 0$  at  $t = 0$  and  $q_t = q_e$  at  $t = t$  equation (13) becomes:

$$q_t = \frac{1}{\beta} \ln(\alpha \beta) + \frac{1}{\beta} \ln(t) \quad (13)$$

If metals ion adsorption fits the Elovich model, a plot of  $q_t$  versus  $\ln(t)$  should yield a linear relationship with a slope of  $1/\beta$  and an intercept of  $1/\beta \ln(\alpha \beta)$ . Figure 9A show a plot of linearization form of Elovich model at constant concentrations studied. The correlation coefficients for the Elovich kinetic model obtained at all the studies were low. This suggests that this adsorption system is not an acceptable for this system.

- **Pseudo First-order Model**

The sorption kinetics may be described by a pseudo first order equation [10]. The linear form equation is the following:

$$\log(q_e - q_t) = \log(q_e) - k_1 t \quad (14)$$

Where,  $q_e$  and  $q_t$  are amounts of dye adsorbed at equilibrium and at time (mg/g), respectively, and  $k$  is the equilibrium rate constant of pseudo first-order adsorption, (1/min). Figure 9B show a plot of linearization form of pseudo first-order model. The slope and intercept of plot of versus was used to determine the pseudo first-order constant and equilibrium adsorption density. However, the experimental data deviated considerably from the theoretical data. A comparison of the results with the correlation coefficients is shown in Figure 9C. The correlation coefficients for the pseudo-first-order kinetic model obtained were low. This suggests that this adsorption system is not a pseudo first-order reaction.

- **Pseudo Second-order Model**

The adsorption kinetics may also be described by a pseudo second-order equation [40]. The linear form equation is the following:

$$\frac{t}{q_t} = \frac{1}{k_2 q_e^2} + \frac{t}{q_e} \quad (15)$$

Where  $k_2$  is the equilibrium rate constant of pseudo second-order adsorption (g/mg.min). The slope and intercept of plot  $t/q$  versus  $t$  was used to calculate the pseudo second-order rate constant  $k_2$  and  $q_e$ . The straight lines in plot of  $t/q$  versus  $t$

(Figure 9C) show good agreement of experimental data with the pseudo second-order kinetic model for different temperature on adsorption process evaluated from 298 to 318 K. Table 2 lists the computed results obtained from the pseudo second-order kinetic model. These indicate that the adsorption system studied belongs to the second order kinetic model.

- **The Intra-particle Diffusion Model**

The intra-particle diffusion model is expressed as [25]:

$$q = k_i t^{1/2} + C \quad (16)$$

where C is the intercept and  $k_i$  is the intra-particle diffusion rate constant ( $\text{mg/g h}^{0.5}$ ), which can be evaluated from the slope of the linear plot of  $q$  versus  $t^{1/2}$ . Figure 9D shows a plot of the linearized form of the intra-particle diffusion model. As can be seen from these figures, the pseudo first-order kinetic model provides the best

correlation for all of the adsorption process, whereas the other models fits the experimental data well not for initial periods of the adsorption process only. Hence it was concluded that the pseudo second-first kinetic model was found to be rate limiting. The rate constant of the pseudo second-order model could be expressed as a function of temperature by the Arrhenius relationship using Eq. (17) [41]:

$$\ln k_2 = \ln A - \frac{E_a}{RT} \quad (17)$$

Where  $k_2$  is the rate constants of the pseudo second-order model ( $\text{min}^{-1}$ ), A is the Arrhenius constant,  $E_a$  is the activation energy ( $\text{kJ mol}^{-1}$ ), R is the universal gas constant ( $8.314 \text{ J } ^\circ\text{K}^{-1} \text{ mol}^{-1}$ ) and T is the absolute temperature ( $^\circ\text{K}$ ). The activation energy can be calculated from the slope of a plot of  $\ln(k_2)$  versus  $1/T$  at three temperatures (298, 308, 318  $^\circ\text{K}$ ) (Figure 10).

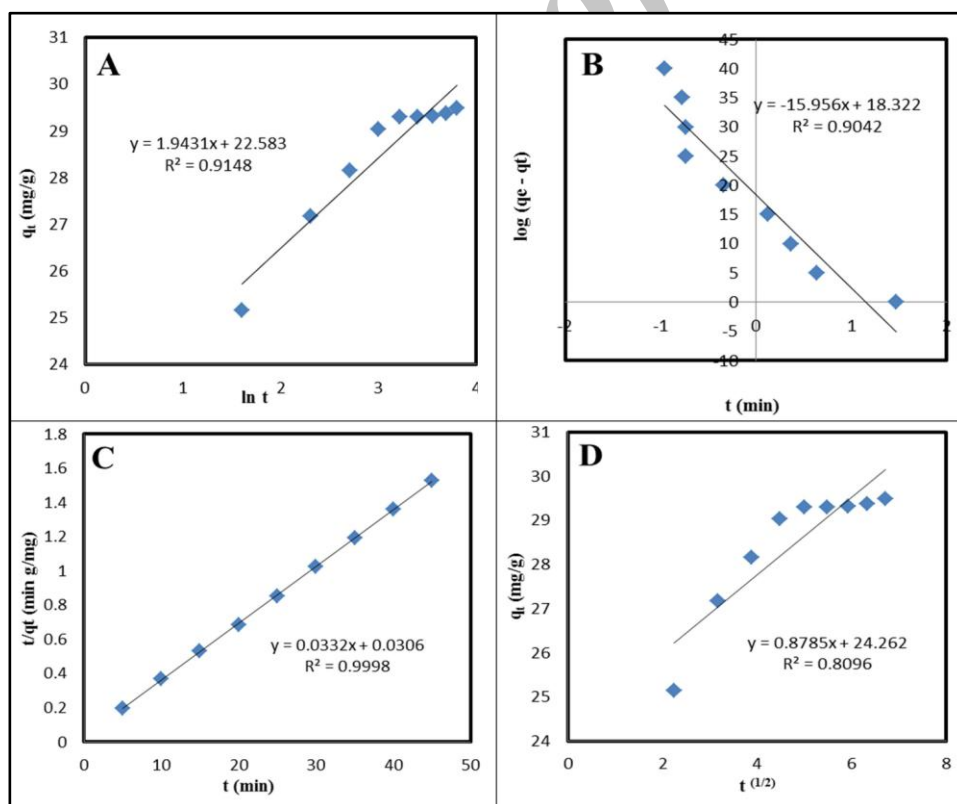


**Fig.9.** (A) Plot of the Elovich adsorption kinetic of MO dye on MWCNT-COOH. (B) Plot of the Pseudo First-order adsorption kinetic of MO dye on MWCNT-COOH. (C) Plot of the Pseudo Second-order adsorption kinetic of MO dye on MWCNT-COOH. (D) Plot of the Intra-particle Diffusion adsorption kinetic of MO dye on MWCNT-COOH. Conditions:  $C_0$ : 20 mg/L of dye solution; mass of adsorbent: 20 mg; the temperature: 298 K and time: 5-45 min at pH 2.

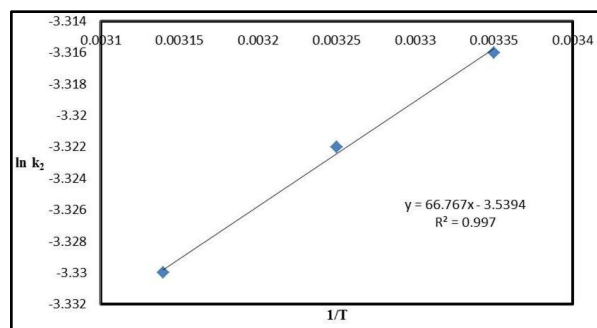


Fig. 10. The plot of  $\ln k_2$  vs.  $1/T$  for the adsorption of MO dye on MWCNT-COOH, using the Arrhenius equation.

### Desorption experiment

In order to check the reuse of the MWCNT-COOH as adsorbent for the adsorption of MO dye, It has been reported in the literature that the best elution efficiency was obtained with the mixture methanol + 4.0 mol L<sup>-1</sup> NaOH [23]. The MO dye at pH 2.0 is attracted electro statically by the MWCNT-COOH. This interaction was corrupted with the NaOH solution. However, besides this electrostatic interaction, there are also some interactions between the aromatic groups present on the MWCNT-COOH with the aromatic rings of the dye. For breaking of this interaction, it was required methanol to improve the elution efficiency which attained up to 81.37% with the mixture methanol + 4.0 mol L<sup>-1</sup> NaOH. On the other hand the MWCNT-COOH, eluted with the mixture methanol + 4.0 mol L<sup>-1</sup> was reutilized for the adsorption of the MO dye, attaining a sorption efficiency of about 78% in the second cycle, 75% in the third cycle of adsorption/desorption when compared with the first cycle of adsorption/desorption. Therefore, the use of MWCNT-COOH for dye adsorption could be economically viable since it allows its regeneration. In addition, there is a tendency for decreasing the prices of CNT with their industrial production growth in the last years [42].

### CONCLUSIONS

Carboxylate group functionalized multi-walled carbon nanotube (MWCNT-COOH) was good adsorbent to removal Reactive methyl orange (MO) textile dye from aqueous solutions. The

adsorbent materials were characterized by FTIR spectroscopy and SEM.

The MO dye interacted with the MWCNT-COOH adsorbent at the solid/liquid interface when suspended in water. The best conditions were established with respect to pH and contact time to saturate the available sites located on the adsorbent surface. Four kinetic models were used to adjust the adsorption, and the best fit was the pseudo second-order kinetic model. The activation energy of the adsorption process was calculated by performing kinetic analysis at different temperatures (298-323 °K). The equilibrium isotherm of the MO dye was obtained, and these data fit best to the Langmuir isotherm model. The MWCNT material loaded with MO dye could be regenerated efficiently using a mixture methanol + 4 mol L<sup>-1</sup> NaOH.

### REFERENCES

- [1] Forgacs E., Cserhati T., Oros G., (2004), Removal of synthetic dyes from wastewaters hydroxide sludge as adsorbent: A review. *Env. Int.* 30: 953–971.
- [2] Santos S. C. R., Vilar V. J. P., Boaventura R. A. R., (2008), Waste metal for a reactive dye. *J. Hazar. Mater.* 153: 999–1008.
- [3] Brookstein D. S., (2009), Factors associated with textile pattern dermatitis caused by contact allergy to dyes, finishes, foams, and preservatives. *Dermato. Clin.* 27: 309-322.
- [4] De Lima R. A., Bazo A. P., Salvadori D. M. F., Rech C. M., Oliveira D. P., Umbuzeiro G. A., (2007), Mutagenic and carcinogenic potential of a textile azo dye processing plant effluent that impacts a drinking water source. *Mutat. Res. Genet. Toxicol. Environ. Mutagen.* 626: 53-60.
- [5] Carneiro P. A., Umbuzeiro G. A., Oliveira D. P., Zanoni M. V. B., (2010), Assessment of water contamination caused by a mutagenic textile effluent dyehouse bearing disperse dyes. *J. Hazar. Mater.* 174: 694-699.

- [6] Gonçalves I. M., Ferrá M. I., Amorim M. T. P., (1996), Processos de remoção biológica de corantes nos efluentes de indústria têxtil. *Tecnologias do Ambiente*. 11: 35–38.
- [7] Sun Q. Y., Yang L. Z., (2003), The adsorption of basic dyes from aqueous solution on modified peat-resin particle. *Water. Res.* 37: 1535–1544.
- [8] Onal Y., (2006), Kinetics of adsorption of dyes from aqueous solution using activated carbon prepared from waste apricot. *J. Hazard. Mater.* 137: 1719–1728.
- [9] Saleh T. A., Gupta V. K., (2012), Photocatalyzed degradation of hazardous dye methyl orange by use of a composite catalyst consisting of multi-walled carbon nanotubes and titanium dioxide. *Colloid. Interface. Sci.* 371: 101–106.
- [10] Robati D., Fakhri A., (2012), Modeling of the adsorption kinetics of Basic Red 46 on single-walled carbon nanotube and carboxylate group functionalized single-walled carbon nanotube. *Phys. Theor. Chem. IAU Iran*. 9: 125–133.
- [11] Lu C., Chiu H., (2006), Adsorption of Zinc(II) from water with purified carbon nanotubes. *Chem. Eng. Sci.* 61: 1138–1145.
- [12] Li Y. H., Wang S., Luan Z., Ding J., Xu C., Wu D., (2003), Adsorption of cadmium (II) from aqueous solution by surface oxidized carbon nanotubes. *Carbon*. 41: 1057–1062.
- [13] Li Y. H., Wang S., Wei J., Zhang X., Xu C., Luan Z., Wu D., Wei B., (2002), Lead adsorption on carbon nanotubes. *Chem Phys. Lett.* 357: 263–266.
- [14] Al-Asheh S., Banat F., Mobai F., (1999), Sorption of copper and nickel by spent animal bones. *Chemosphere*. 39: 2087–2096.
- [15] Lin S. H., Lai S. L., Leu H. G., (2000), Removal of heavy metals from aqueous solution by chelating resin in a multistage adsorption process. *J. Hazard. Mater.* B76: 139–153.
- [16] Li Y. H., Wang S., Wei J., Zhang X., Wei J., Xu C., Luan Z., Wu D., (2003), Adsorption of fluoride from water by aligned carbon nanotubes. *Mater. Res. Bull.* 38: 469–476.
- [17] Zhou L., Zhang X., Yang H., Peng B., (2009), Adsorption and Ability to Carry Catalysts of Carbon Nanotubes for Destructing Dioxins. *Mater. Scienc.* 2: 226–231.
- [18] Roberts J. D., Caserio M. C., (1977), Basic Principles of Organic Chemistry, second ed. W.A. Benjamin Incorporation, London.
- [19] Vaghetti J. C. P., Lima E. C., Royer B., Brasil J. L., Cunha B. M., Simon N. M., Cardoso N. F., Norena C. P. Z., (2008), Application of Brazilian-pine fruit coat as a biosorbent to removal of Cr(VI) from aqueous solution. Kinetics and equilibrium study. *Biochem. Eng. J.* 42: 67–76.
- [20] Cardoso N. F., Lima E. C., Pinto I. S., Amavisca C. V., Royer B., Pinto R. B., Alencar W. S., Pereira S. F. P., (2011), Application of cupuassu shell as biosorbent for the removal of textile dyes from aqueous solution. *J. Environ. Manage.* 92: 1237–1247.
- [21] Cardoso N. F., Pinto R. B., Lima E. C., Calvete T., Amavisca C. V., Royer B., Cunha M. L., Fernandes T. H. M., Pinto I. S., (2011), Removal of remazol black B textile dye from aqueous solution by adsorption. *Desalination*. 269: 92–103.
- [22] Smith B., (1999), Infrared Spectral Interpretation. A Systematic Approach, CRC Press, Boca Raton.
- [23] Machado F. M., Bergmann C. P., Fernandes T. H. M., Lima E. C., Royer B., Calvete T., Fagan S. B., (2011), Adsorption of Reactive Red M-2BE dye from water solutions by multi-walled carbon nanotubes

- and activated carbon. *Hazar. Mater.* 192: 1122–113.
- [24] Ali Atieh M., Yehya Bakather O., (2010), Effect of Carboxylic Functional Group Functionalized on Carbon Nanotubes Surface on the Removal of Lead from Water, *Bioinorga. Chem. Appli.* Article. ID 603978, 9 pages.
- [25] Calvete T., Lima E. C., Cardoso N. F., Vaghetti J. C. P., Dias S. L. P., Pavan F. A., (2010), Application of carbon adsorbents prepared from Brazilian-pine fruit shell for the removal of reactive orange 16 from aqueous solution: kinetic, equilibrium, and thermodynamic studies. *J. Environ. Manage.* 91: 1695–1706.
- [26] Cardoso N. F., Lima E. C., Pinto I. S., Amavisca C. V., Royer B., Pinto R. B., Alencar W. S., Pereira S. F. P., (2011), Application of cupuassu shell as biosorbent for the removal of textile dyes from aqueous solution. *J. Environ. Manage.* 92: 1237–1247.
- [27] Vaghetti J. C. P., Lima E. C., Royer B., Cunha B. M., Cardoso N. F., Brasil J. L., Dias S. L. P., (2009), Pecan nutshell as biosorbent to remove Cu(II), Mn(II) and Pb(II) from aqueous solutions. *J. Hazar. Mater.* 162: 270–280.
- [28] El-Khaiary M. I., Malash G. F., (2001), Common data analysis errors in batch adsorption studies. *Hydrometallurgy.* 105: 314–320.
- [29] Chen A. H., Chen S. M., (2009), Biosorption of azo dyes from aqueous solution by glutaraldehyde-cross linked chitosans. *J. Hazard. Mater.* 172: 1111–1121.
- [30] Ertugay N., Bayhan Y. K., (2010), The removal of copper (II) ion by using mushroom biomass (*Agaricusbisporus*) and kinetic modelling. *Desalination.* 255: 137–142.
- [31] Lopes E. C. N., Anjos F. S. C., Vieira E. F. S., Cestari A. R., (2003), An alternative Avrami equation to evaluate kinetic parameters of the interaction of Hg(II) with thin chitosan membranes. *J. Colloid. Interface. Sci.* 263: 542–547.
- [32] Largegren S., (1898), About the theory of so-called adsorption of soluble substances. *K. Sven. Vetenskapsakad. Handl.* 24: 1–39.
- [33] Ho Y. S., Mckay G. M., (1999), Pseudo-second order model for sorption process. *Biochem.* 34: 451–465.
- [34] Weber Jr. W. J., Morris J. C., (1963), Kinetics of adsorption on carbon from solution. *J. Sanit. Eng. Div. Am. Soc. Civil Eng.* 89: 31–59.
- [35] Langmuir I., (1918), The adsorption of gases on plane surfaces of glass, mica and platinum. *J. Am. Chem. Soc.* 40: 1361–1403.
- [36] Freundlich H., (1906), Adsorption in solution. *Phys. Chem. Soc.* 40: 1361–1368.
- [37] Lima E. C., Royer B., Vaghetti J. C. P., Brasil J. L., Simon N. M., Santos-Jr A. A. dos, Pavan F. A., Dias S. L. P., Benvenuti E. V., Silva E. A. da, (2007), Adsorption of Cu(II) on *Araucaria angustifolia* wastes: Determination of the optimal conditions by statistic design of experiments. *J. Hazar. Mater.* 140: 211–220.
- [38] Upadhyayula V. K. K., Deng S., Mitchell M. C. G. B., (2009), Smith application of carbon nanotube technology for removal of contaminants in drinking water: A review. *Sci. Total Environ.* 408: 1–13.
- [39] Moradi O., (2012), Applicability comparison of different models for ammonium ion adsorption by multi-walled carbon nanotube. *Arab. J. Chem.* 1-7.
- [40] Vaghetti J., Lima E., Royer B., Cunha B. da, Cardoso N., Brasil J., Dias S. (2009), Pecan nutshell as biosorbent to remove Cu(II), Mn(II) and Pb(II) from aqueous solutions. *J. Hazar. Mater.* 162: 270–280.



- [41] Maleki M., Moradi O., Tahmasebi S., (2012), Adsorption of albumin by gold nanoparticles, Equilibrium and thermodynamics studies. Arab. J. Chem. In Press.
- [42] Agboola A., Pike R., Hertwig T., Lou H., (2007), Conceptual design of carbon nanotube processes. *Clean. Technol. Environ. Policy*. 9: 289–311.
- [43] Webber T., Chakkravorti R., (1974), Pore and solid diffusion models for fixed-bed adsorbers. *AIChE J.* 20: 228–238.
- [44] Ozcan A., Erdem S., Ozcan B., (2004), Adsorption of acid blue 193 from aqueous solutions onto Na-bentonite and DTMA-bentonite. *J. Colloid. Interface Sci.* 280: 44–54.
- [45] Temkin M., Pyzhev V., (1940), Recent modifications to Langmuir isotherms. *Acta Physiol. Chem. USSR*. 12: 217-222.

Cite this article as: M. Rajabi et al.: Adsorption of Methyl orange dye from Water solutions by carboxylate group functionalized multi-walled Carbon nanotubes.  
*Int. J. Nano Dimens.* 6(3): 227-240, Summer 2015.